AIP | Journal of Applied Physics

Surface bulk differences in a conventional superconductor, ZrB12

Sangeeta Thakur, Deepnarayan Biswas, Nishaina Sahadev, P. K. Biswas, G. Balakrishnan et al.

Citation: J. Appl. Phys. **114**, 053904 (2013); doi: 10.1063/1.4817415
View online: http://dx.doi.org/10.1063/1.4817415
View Table of Contents: http://jap.aip.org/resource/1/JAPIAU/v114/i5
Published by the AIP Publishing LLC.

JOURNAL OF APPLIED PHYSICS **114**, 053904 (2013)

Surface bulk differences in a conventional superconductor, ZrB_{12}

Sangeeta Thakur,[1] Deepnarayan Biswas,[1] Nishaina Sahadev,[1] P. K. Biswas,[2,a)] G. Balakrishnan,[2] and Kalobaran Maiti[1,b)]
[1]*Department of Condense Matter Physics and Materials Science, Tata Institute of Fundamental Research, Colaba, Mumbai-400005, India*
[2]*Department of Physics, University of Warwick, Coventry CV4 7AL, United Kingdom*

(Received 10 July 2013; accepted 18 July 2013; published online 2 August 2013)

We studied the electronic structure of a conventional superconductor, ZrB_{12}, using high resolution x-ray photoemission spectroscopy and single crystalline samples. Experimental results with different bulk sensitivity reveal boron deficiency at the surface while the bulk is stoichiometric and different valence states of Zr at the surface relative to those in the bulk. Signature of satellite features is observed in the Zr core level spectra corresponding to the bulk of the material suggesting importance of electron correlation among the conduction electrons in the bulk while the surface appears to be uncorrelated. These results provide an insight on surface-bulk differences, which is important for fabrication of devices based on such superconductors. © *2013 AIP Publishing LLC*. [http://dx.doi.org/10.1063/1.4817415]

I. INTRODUCTION

Superconductors play an important role in technological applications including various medical tools and are potential candidates for future applications such as lossless power transmission, maglev trains, etc. Fabrication of devices requires good knowledge of the surface and bulk properties, which are often found to be different in many systems.[1] Here, we considered a conventional superconductor, ZrB_{12}; the electronic properties of these systems are well captured by the Bardeen-Cooper-Schriefer (BCS) theory and come among the simplest cases of the superconducting materials.

ZrB_{12} exhibits highest superconducting transition temperature ($T_c \sim 6$ K) in MB_{12} family.[2] In the crystal, Zr atoms are surrounded by 24 boron atoms arranged on a truncated octahedron and has the smallest lattice constant (space group[3,4] $Fm3m$, $a = 7.4075$ Å) of all known dodecaborides.[5] Scanning tunneling spectroscopy and magnetization measurements show that ZrB_{12} single crystal has excellent surface properties.[6] Enthalpy measurements[7] in $Zr_{0.6}Y_{0.4}B_{12}$ suggest the most probable valence state of Zr to be (+4). In contrast, the x-ray photoemission (XP) spectroscopic measurements on polycrystalline ZrB_{12} sample indicate neutral state of Zr; the earlier observation of (+4) valence state is attributed to the impurity phase. Clearly, the microscopic details of the electronic properties remain to be puzzling and require high resolution studies as observed in other complex systems.[8]

We employed high resolution x-ray photoemission spectroscopy to investigate the electronic structure of single crystalline samples of ZrB_{12}. X-rays of varied photon energies ranging till hard x-ray regime provide wide ranging surface sensitivity in the photoemission spectroscopic technique. The experimental results as a function of surface sensitivity reveal interesting differences in the bulk and surface electronic structures of this material.

II. EXPERIMENT

Single crystals of ZrB_{12} were grown by floating zone technique as described elsewhere.[9] The photoemission measurements were performed using a Gammadata Scienta R4000 WAL analyzer and monochromatic Al $K\alpha$ radiations ($h\nu_1 = 1486.6$ eV) with the energy resolution set to 400 meV. Hard x-ray photoemission measurements were carried out at P09 beam line, PETRA III Hamburg, Germany with 5947.9 eV ($h\nu_2$) photon energy and an electron analyzer from Specs GmbH with the energy resolution set to 150 meV. The melt grown single crystals were hard and have no cleavage plane. Therefore, we followed surface cleaning procedures such as fracturing using a post on the sample as well as scraping using a diamond file in the vacuum chamber with vacuum better than 3×10^{-11} Torr. After sample surface preparation in the ultra-high vacuum chamber, it was transported to the experiment chamber without exposing to atmosphere so that the surface remains clean for the photoemission measurements. The angle integrated spectra collected in transmission mode with large acceptance angle were found to be reproducible after each of the surface cleaning cycles and no signature of impurity was found in the spectra. The temperature variation down to 10 K was achieved by an open cycle He cryostat from Advanced Research systems, USA.

III. RESULTS AND DISCUSSION

The Zr $3d$ core level spectra were probed using 1486.6 eV ($= h\nu_1$) and 5947.9 eV ($= h\nu_2$) photon energies. The photoelectron escape depth, λ (=the distance traveled by the photoelectrons without inelastic scattering), can be varied by varying the incident photon energy.[1] The value of λ of the conduction electrons is close to 20 Å for $h\nu_1$ and about 40 Å for $h\nu_2$. Assuming $\lambda \propto \sqrt{KE}$ at higher kinetic energies (KE), λ for Zr $3d$ electrons would be 18.7 Å and

a)Present address: Paul Scherrer Institut, CH-5232 Villigen PSI, SWITZERLAND.
b)Author to whom correspondence should be addressed. Electronic mail: kbmaiti@tifr.res.in

39.5 Å for $h\nu_1$ and $h\nu_2$, respectively. Thus, at $h\nu_2$, the photoemission spectrum essentially represents the bulk electronic structure of the sample.

The Zr 3*d* and B 1*s* core level spectra collected using $h\nu_1$ and $h\nu_2$ are shown in Fig. 1. At $h\nu_1$, the B 1*s* feature exhibits a sharp asymmetric shape as expected in a metallic system. The integrated intensity of the B 1*s* feature relative to the integrated Zr 3*d* signal increases significantly at $h\nu_2$ along with an additional feature, D around 187 eV binding energy and increased intensity at higher binding energy side (feature F). An increase in intensity ratio $[I(B1s)/I(Zr4d)]$ by about 1.5 times is expected due to the change in photoemission cross-sections of the corresponding energy levels. However, the experimental spectra in Fig. 1 exhibit an increase by about 2.7 times in the present case. Such substantial increase in intensity at the larger probing depth suggests B deficiency at the surface. This effect is found to be independent of the surface preparation consistent with earlier results on single crystal surface cut by diamond saw without chemical etching of the damaged surface layer.[10] Such boron deficiency at the surface can arise due to the poorer sticking of borons at the top of the huge B_{12} cages at the surface.

The Zr 3*d* spectral region (179–186 eV) exhibits multiple distinct features denoted by A1, A2, B1, B2, C1, and C2 in Figs. 1 and 2 are used for $3d_{5/2}$ and $3d_{3/2}$ signals, respectively. The spin-orbit splitting is found to be about 2.3 eV. The intensities of the features change significantly with the change in surface sensitivity of the technique indicating significantly different surface and bulk electronic structure. At $h\nu_2$, the intensity of the features, B1 and B2 become almost insignificant, although it has large intensity in the $h\nu_1$ spectrum indicating surface nature of these peaks. The features, A1 and A2, reduce in intensity in the bulk sensitive $h\nu_2$ spectrum. Evidently, the bulk electronic structure is dominated by the contributions from the features C1 and C2. Two additional features S1 and S2 are also observed in the spectra—the intensity of these features becomes stronger in the bulk sensitive $h\nu_2$ spectrum again suggesting their bulk nature.

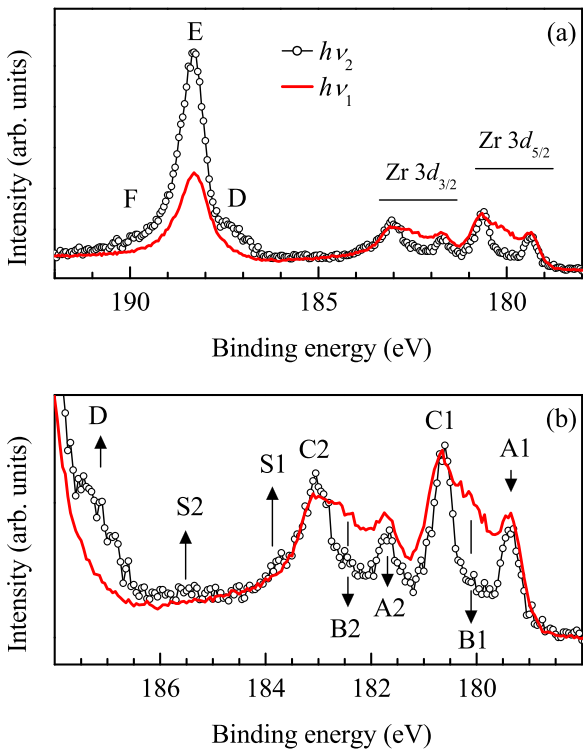

FIG. 1. (a) Zr 3*d* core level spectra of ZrB_{12} using 1486.6 eV ($h\nu_1$) and 5947.9 eV ($h\nu_2$) photon energies. Photoemission spectra exhibit distinct signature of satellites. (b) Zr 3*d* spectral region is shown with enhanced *y*-scale.

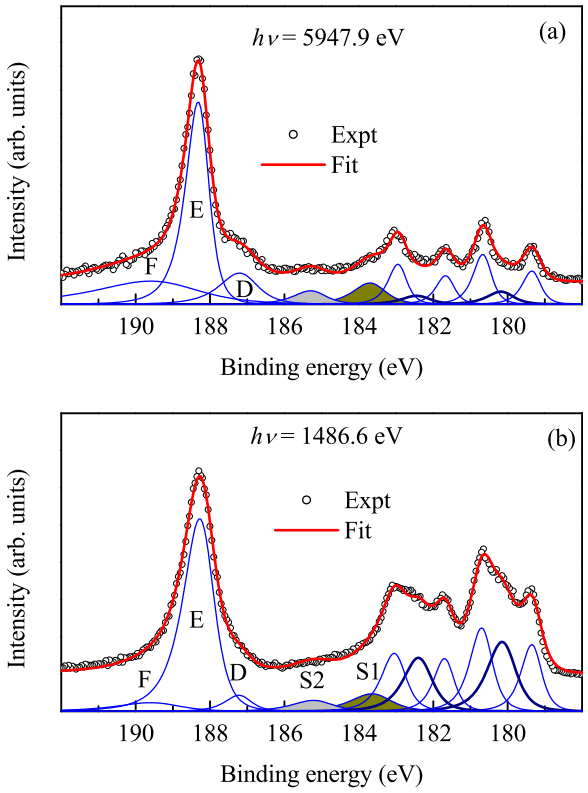

FIG. 2. Fits of the core level spectra collected using (a) 1486.6 eV and (b) 5947.9 eV photon energies. The component peaks are shown by solid lines.

To determine the energy position and relative weight of the spectral features, we have fit the experimental spectra with a set of asymmetric Doniach-Šunjić-type lineshapes,[11] which is expected in metallic samples due to low energy excitations across ϵ_F in the photoemission final states. Three distinct features in each of the spin-orbit split signals were represented by three peaks as shown in Fig. 2 and the spin-orbit splitting is set at the experimental value of 2.3 eV. The least square error fitting method provides the intensity ratio of the spin orbit split features close to their multiplicity.

The thick solid lines superimposed over the experimental data in Fig. 2 exhibit good representation of the experimental spectra. The binding energies of the features A1 and C1 are found to be 179.4 eV and 180.7 eV—these energies correspond well with the 3*d* peak positions observed for Zr^0 and Zr^{2+} species, respectively. This is different from the spectra observed from polycrystalline samples containing signature of boron oxides.[12] Such multiple valencies of Zr have been observed in Zr halides, oxides,[13–15] and other dodecaborides, YbB_{12}, UB_{12}, etc., as well.[7,16] The binding energy of the feature B1 is found to be about 180.2 eV, which corresponds to Zr^+.

Evidently, the results on ZrB_{12} reveal unusual mixed valency of Zr—different kinds of mixed valency at the surface and bulk of the sample. The $h\nu_1$ spectrum exhibits distinct signature of the feature "B"s corresponding to Zr^+ species (thick solid lines in the figure) and a larger intensities of the features "A"s relative to the intensities of "C"s. This suggests large contributions from Zr^0 and Zr^+ at the surface while the bulk is dominated by Zr^{2+} contributions along with Zr^0 contributions. Zr^+ possessing electronic configuration of [Kr]4 $d^2$5 s^1 is not a stable configuration and hence is unstable in the bulk. Any such entity would charge disproportionate to Zr^0 and Zr^{2+}.[17] The boron deficiency at the surface provides a reconstructed electronic structure stabilizing the Zr^+ entities.

The features S1 and S2 (see Figs. 1 and 2) exhibit the energy separation close to 2.3 eV, which is similar to the spin-orbit splitting. These features could be fit with two peaks marked S1 and S2 in Fig. 2 and are attributed to the satellite features associated to the photoemission of 3*d* electrons. The other possibility could be loss features due to various collective excitations in the solid such as plasmon excitations, phonon excitations, etc. If that is the case, the signature of such loss features would appear with every core level studied. However, we did not observe this to happen with any of the boron core levels studied. Moreover, the energy separation of such feature in Zr 3*p* spectra shown in Fig. 3 is much larger than 3 eV observed in the 3*d* core level spectra. Thus, one can rule out the possibility of loss features in the present case. The intensity of the satellite feature increases with the increase in bulk sensitivity indicating that these are associated to the bulk electronic structure dominated by Zr^{2+} contributions.

The boron (B 1*s*) core level spectrum also shows an asymmetry towards higher binding energies.[11] The binding energy of B 1*s* is consistent with the reported values in typical transition metal borides[18] and borocarbides RNi_2B_2C (R = Y and La) Ref. 19 (187.1–188.3 eV). We have not observed evidence of impurity phases such as B_2O_3 (B 1*s*; 191.10 eV) in our spectra in contrast to that found earlier in the case of polycrystalline ZrB_{12} sample.[12] Although all the boron sites are equivalent from the crystal structure point of view, observation of three distinct features with significantly different binding energies indicates the presence of more than one type of B in the crystal. The intensity of the feature at 187 eV (feature D in Fig. 2) is more intense in the relatively more bulk sensitive spectra indicating its bulk nature. These boron atoms presumably reside closure to the Zr^{2+} sites with largest effective negative potential leading to a lower binding energy.

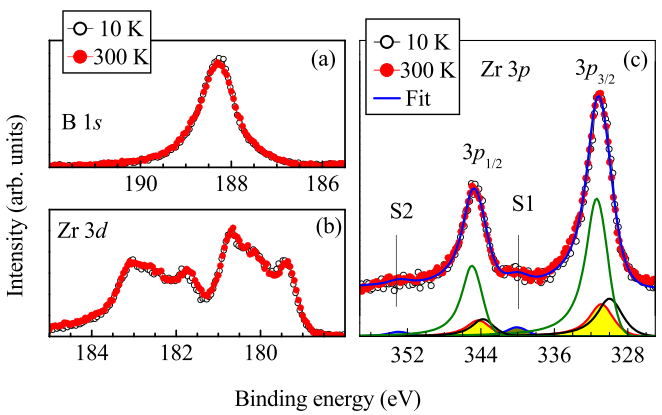

FIG. 3. (a) B 1*s*, (b) Zr 3*d*, and (c) Zr 3*p* core level spectra at 10 K (open circles) and 300 K (closed circles). The lines in (c) show the fitting results.

The spectra collected with $h\nu_1$ photon energy at 300 K and 10 K are superimposed in Fig. 3 to see the effect of temperature. Clearly, the line shape of all the core level spectra remains almost identical at these two widely differed temperatures. Although 10 K is little higher than the superconducting transition temperature, the large change in temperature from 300 K to 10 K expected to manifest the phonon induced effects. Almost identical shape and relative intensity of the features in all the core level spectra suggest that the thermal influence on the electronic structure, if there is any, is below the detection level of the technique. In order to investigate the signature of satellite and temperature effects independently on other core level spectra, we analyze the Zr 3*p* core level spectra in Fig. 3(c). Again, the spectral lineshape is found to be identical at both the temperatures studied. The spectra could be simulated using multiple Zr valencies along with the signature of satellites S1 and S2 associated to the spin-orbit split 3*p* signals reestablishing independently the conclusions from the Zr 3*d* core level spectra.

The atomic number 40 of Zr corresponds to the electronic configuration of [Kr]4 $d^2$5 s^2. Since the B_{12} unit has an effective valency of (2^-),[20] the expected Zr valency in this system would be Zr^{2+} with an electronic configuration of 4 d^2—these two electrons will populate the t_{2g} bands leading to the metallic ground state. Since the satellite feature represents the poorly screened feature in the photoemission spectra, the corresponding electronic state configuration will be $|4d^2>$ in the photoemission final state. The main peak C1 corresponds to the well screened final state, where the positive charge due to the core hole is screened by the transfer of an electron from the conduction band and/or ligands leading to an electronic state $|4d^3\underline{L}>$; $\underline{L}$ represent a hole in the ligand levels. The energy separation, ΔE, of the peak C1 to the satellite feature S1 is about 3 eV. The intensity ratio of the peaks S1 and C1 is in the range of 0.5 to 0.6, which is quite large considering the intensity ratios found in various transition metal oxides such as cuprates.[21] Considering the above discussed two final states representing the electronic spectra within the first approximation, the electron correlation strength is expected to be close to 3 eV.[21,22]

IV. CONCLUSIONS

In summary, we studied the electronic structure of a BCS superconductor, ZrB_{12} employing high resolution photoemission spectroscopy. Hard x-ray photoemission helped to reveal different surface and bulk electronic structure of this compound. Experimental results exhibit large Zr^{2+} component in the bulk along with some Zr^0 component. Multiple valencies of Zr appear at the surface due to boron deficiency in the surface layers. In addition, we observe signature of satellite feature in the Zr core level spectra indicating finite

electron correlation among conduction electrons. Decrease in temperature down to 10 K does not have significant influence in the spectral lineshape and/or energy position indicating the influence from the lattice degrees of freedom is below the detection limit. These results provide evidence of different surface and bulk electronic structure even is a conventional superconductor, ZrB_{12}, which is important to consider while fabricating devices based on these materials.

ACKNOWLEDGMENTS

The authors acknowledge financial support from the DST-DESY project to perform the experiments at P09 beamline at PETRA III, Hamburg, Germany and Dr. Indranil Sarkar for his help during the measurements. The authors, K.M. and N.S. acknowledge the Department of Science and Technology for financial assistance under the Swarnajayanti Fellowship Programme. G.B. wishes to acknowledge financial support from EPSRC, UK (EP/I007210/1).

[1]K. Maiti, U. Manju, S. Ray, P. Mahadevan, I. H. Inoue, C. Carbone, and D. D. Sarma, Phys. Rev. B **73**, 052508 (2006); K. Maiti, A. Kumar, D. D. Sarma, E. Weschke, and G. Kaindl, *ibid.* **70**, 195112 (2004); K. Maiti and D. D. Sarma, *ibid.* **61**, 2525 (2000); K. Maiti and R. S. Singh, *ibid.* **71**, 161102(R) (2005); K. Maiti, R. S. Singh, and V. R. R. Medicherla, *ibid.* **76**, 165128 (2007).
[2]B. T. Matthias, T. H. Geballe, K. Andres, E. Corenzwit, G. W. Hull, and J. P. Maita, Science **159**, 530 (1968).
[3]B. Post and F. W. Glaser, J. Metals Trans. AIME **194**, 631 (1952).
[4]Yu. B. Paderno, A. B. Liashchenko, V. B. Filippov, and A. V. Dukhnenko, *Advantages and Challenges in Science for Materials in the Frontier of Centuries*, edited by V. V. Skorokhod (IPMS, Kiev 347 2002).
[5]Z. Fisk and B. T. Matthias, Science **165**, 279 (1969).
[6]M. I. Tsindlekht, G. I. Leviev, I. Auslin, A. Sharoni, O. Millo, I. Felner, Yu. B. Paderno, V. B. Filipov, and M. A. Belogolovski, Phys. Rev. B **69**, 212508 (2004).
[7]R. W. Mar and N. D. Stout, J. Chem. Phys. **57**, 5342 (1972).
[8]R. Bindu, G. Adhikary, N. Sahadev, N. P. Lalla, and K. Maiti, Phys. Rev. B **84**, 052407 (2011); R. Bindu, S. Singh, N. Singh, R. Ranjan, K. Maiti, A. H. Hill, and S. R. Barman, *ibid.* **86**, 140104(R) (2012).
[9]G. Balakrishnan, M. R. Lees, and D. M. K. Paul, J. Cryst. Growth **256**, 206 (2003).
[10]R. Lortz, Y. Wang, S. Abe, C. Meingast, Yu. B. Paderno, V. Filipov, and A. Junod, Phys. Rev. B **72**, 024547 (2005).
[11]S. Doniach and M. Súnjic, J. Phys. C: Solid State Phys. **3**, 285 (1970).
[12]L. Huerta, A. Duran, R. Falconi, M. Flores, and R. Escamilla, Physica C **470**, 456 (2010).
[13]C. Morant, J. M. Sanz, L. Galan, L. Soriano, and F. Rueda, Surf. Sci. **218**, 331 (1989).
[14]A. F. Wells, in *Structural Inorganic Chemistry*, edited by A. F. Wells (Clarendon, Oxford, 1975).
[15]L. Kumar, D. D. Sarma, and S. Krummacher, Appl. Surface Sci **32**, 309 (1988).
[16]F. Iga, Y. Takakuwa, T. Takahashi, M. Kasaya, T. Kasuya, and T. Sagawa, Solid State Commun. **50**, 903 (1984).
[17]C. M. Varma, Phys. Rev. Lett. **61**, 2713 (1988).
[18]C. L. Perkins, R. Singh, M. Trenary, T. Tanaka, and Y. Paderno, Surf. Sci. **470**, 215 (2001); S. Patil, G. Adhikary, G. Balakrishnan, and K. Maiti, Solid State Commun. **151**, 326 (2011).
[19]K. Kobayashi, T. Mizokawa, K. Mamiya, A. Sekiyama, A. Fujimori, H. Takagi, H. Eisaki, S. Uchida, R. J. Cava, J. J. Krajewski, and W. F. Peck, Jr., Phys. Rev. B **54**, 507 (1996).
[20]H. Werheit, V. Fillipov, K. Shirai, H. Dekura, N. Shitsevalova, U. Schwarz, and M. Armbruster, J. Phys.: Condens. Matter **23**, 065403 (2011).
[21]D. D. Sarma and S. G. Ovchinnikov, Phys. Rev. B **42**, 6817(R) (1990).
[22]A. E. Bocquet, T. Mizokawa, K. Morikawa, A. Fujimori, S. R. Barman, K. Maiti, D. D. Sarma, Y. Tokura, and M. Onoda, Phys. Rev. B **53**, 1161 (1996); K. Maiti, D. D. Sarma, T. Mizokawa, and A. Fujimori, Europhys. Lett. **37**, 359 (1997); K. Maiti, P. Mahadevan, and D. D. Sarma, Phys Rev B **59**, 12457 (1999).